Photocontrolled nucleobase binding to an organometallic Ru^{II} arene complex

Soledad Betanzos-Lara, Luca Salassa, Abraha Habtemariam and Peter J. Sadler*

Department of Chemistry, University of Warwick, Coventry, UK CV4 7AL

Supporting Information

Preparation and Characterisation [(η^6-*p*-cym)Ru(bpm)py][PF_6]$_2$ (1a). Using an aluminium foil covered flask at room temperature [(η^6-*p*-cymene)Ru(bpm)Cl][PF_6] (0.10 g, 0.17 mmol) and $AgNO_3$ (0.03 g, 0.17 mmol) in 10 mL of a 1:1 mixture of MeOH/H_2O were heated under reflux for 1 h. AgCl was removed by filtration. A large excess (ca. 25 mol equiv) of pyridine (350 μL, 4.35 mmol) was added, and the mixture was left stirring overnight. The volume was reduced by rotary evaporation and a 5 mol equiv excess of KPF_6 (0.16 g, 0.85 mmol) was added. The precipitate that formed was filtered off and washed with portions of Et_2O and dried overnight in vacuum resulting in a yellow-to-green microcrystalline product.
[(η^6-*p*-cym)Ru(bpm)py][PF_6]$_2$ (**1**): yield 72% (0.09 g, 0.12 mmol). ESI-MS: 236.0 [M^{2+}]. ^{1}H NMR (D_2O, 500 MHz,) δ_H ppm: 0.94 (6H, d, *J* = 6.96), 1.85 (3H, s), 2.48 (1H, sep), 6.18 (2H, d, *J* = 6.53), 6.49 (2H, d, *J* = 6.53 Hz), 7.44 (2H, m), 7.94 (1H, m), 8.15 (2H, m), 8.41 (2H, dd, *J* = 1.31 , J = 6.39), 9.29 (dd, 2H, *J* = 1.90 Hz, *J* = 4.88 Hz), 10.05 (dd, 2H, *J* = 1.95 Hz, *J* = 5.86). ^{13}C NMR (600 MHz,) δ_C ppm: 17.1, 21.5, 25.6, 30.7, 85.9, 90.6, 107.2, 108.0, 126.1, 127.4, 140.1, 153.8, 161.0, 161.4, 163.7.

[(η^6-*p*-cym)Ru(bpm)(H_2O)][PF_6]$_2$ (1b). Using an aluminium foil covered flask at room temperature, [(η^6-*p*-cym)Ru(bpm)Cl][PF_6] (0.10 g, 0.17 mmol) and $AgNO_3$ (0.03 g, 0.17 mmol) were dissolved in 10 mL of a 1:1 mixture of MeOH/H_2O and stirred overnight; the solution turned from bright to dark green. The volume was reduced by rotary evaporation and a 5 mol equiv excess of KPF_6 (0.16 g, 0.85 mmol) was added. The precipitate that formed was filtered off and washed with portions of Et_2O and dried overnight in vacuum resulting in a yellow-to-green microcrystalline product; yield 82% (0.09 g, 0.14 mmol). HR-MS: 411.08 [M^{2+}]. ^{1}H NMR (D_2O, 500 MHz) δ_H ppm: 1.09 (6H, d, *J* = 7.14 Hz), 2.12 (3H, s), 2.66 (1H, sep), 6.15 (2H, d, *J* = 6.67 Hz), 6.37 (2H, d, *J* = 6.75 Hz), 8.15 (t, 2H, *J* = 5.50), 9.29 (2H, dd, *J* = 1.84 Hz, *J* = 5.10 Hz), 10.00 (2H, dd, *J* = 1.84 Hz, *J* = 5.87 Hz).

Instrumentation

NMR Spectroscopy. ^{1}H NMR spectra were acquired on a Bruker DMX 600 spectrometer (^{1}H = 600 MHz). All data processing was carried out using XWIN NMR, version 2.0 (Bruker U.K. Ltd.). ^{1}H NMR signals were referenced dioxan as an internal reference (δ 3.75).

High Resolution Electrospray Mass Spectrometry. HR-MS were obtained on a Bruker MaXis UHR-TOF, all the samples were analysed by ESI(+) at 2uL/min, neubuliser gas 0.4bar, dry gas 4L/min and dry temp 180 degree, Funnel RF 200V, Multiple RF 200, quadrupole ion energy 4 eV, collision cell 5 eV, ion cooler RF settings, ramp from 50 to 250 V.

UV-vis Absorption Spectroscopy. UV-vis absorption spectra were recorded on a Cary 50-Bio spectrophotometer using 1-cm path -length quartz cuvettes (0.5 mL) and a PTP1 Peltier temperature controller. Spectra were recorded at ca. 310 K in double distilled water from 800 to 230 nm, and were processed using UV-Winlab software for Windows 95.

pH* Measurement. pH* values (pH meter reading without correction for effects of D on glass electrode) of NMR samples of compound **1** in D_2O were measured at ca. 298 K directly in the NMR tube, before and after irradiation, using a Corning 240 pH meter equipped with a micro combination electrode calibrated with Sigma-Aldrich buffer solutions at pH 4, 7, and 10.

Figure S1. ^{1}H-^{1}H TOCSY 2D NMR spectrum for an irradiated solution of [(p-cymene)Ru(bpm)(py)]$^{2+}$ in D_2O (aromatic region). Irradiation details: white light (400–600 nm, 1 J/cm^{2}·h) at 310 K for ca. 420 min.

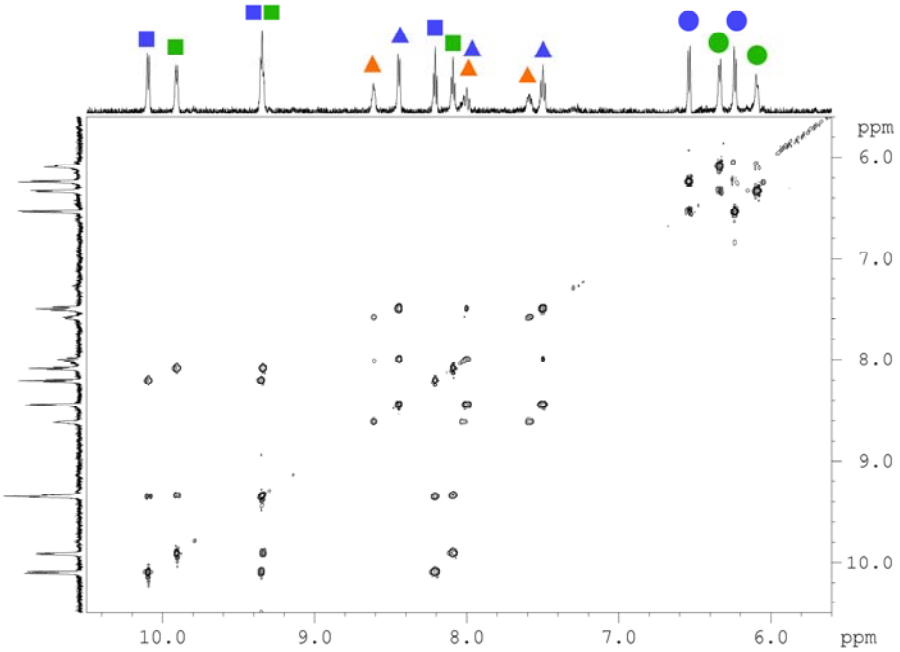

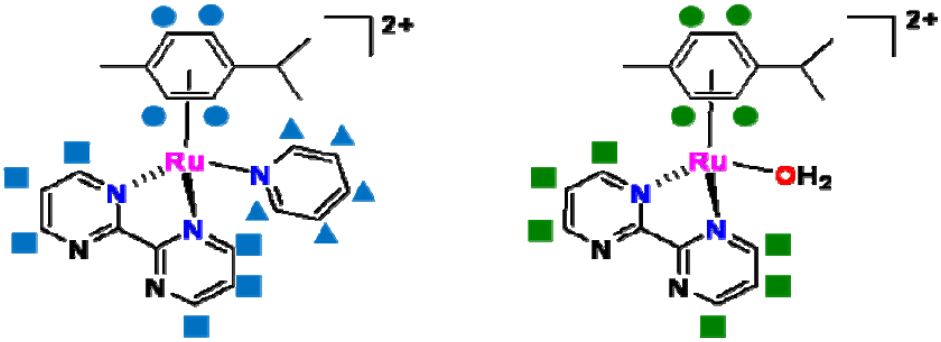

1a **1b**

Free pyridine is indicated with **orange ▲**

Figure S2. ^{1}H-^{1}H TOCSY 2D NMR spectrum for an irradiated solution of [(p-cymene)Ru(bpm)(py)]$^{2+}$ + 9-ethylguanine in D_2O (aromatic region).). Irradiation details: white light (400–600 nm, 1 J/cm^{2}·h) at 310 K for ca. 360 min.

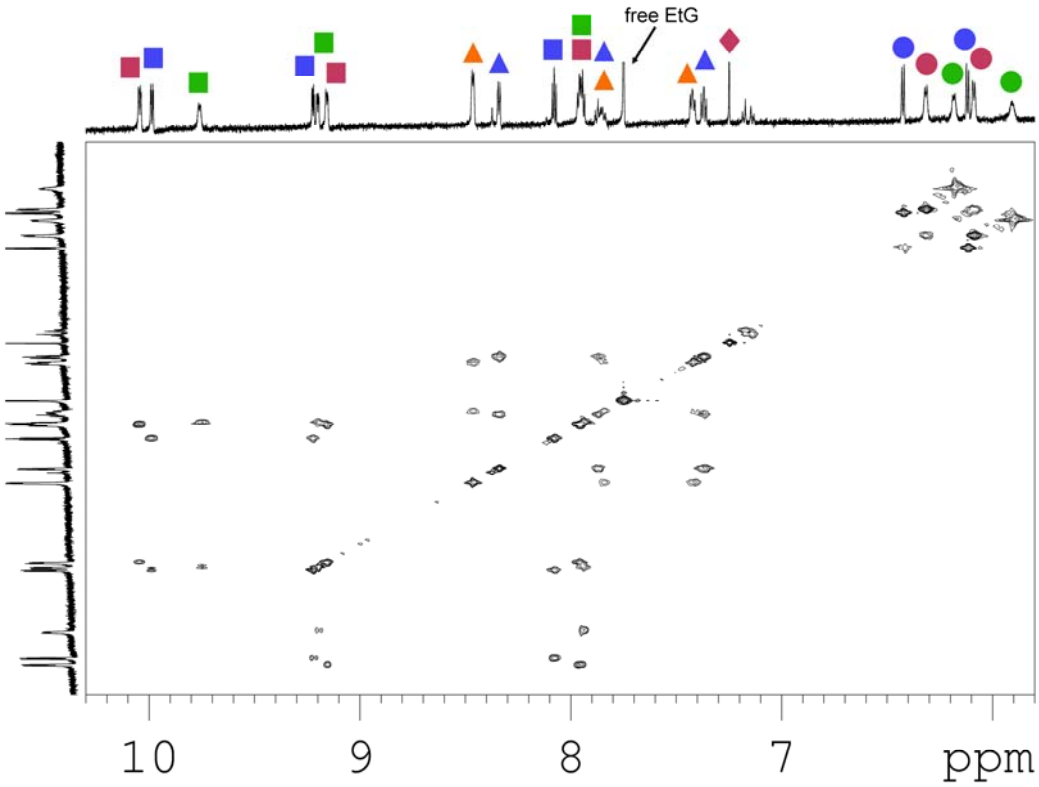

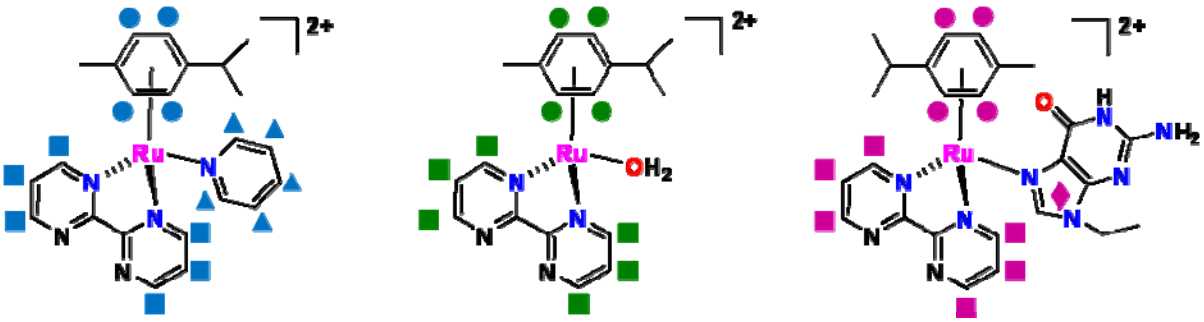

1a **1b** **1c**

Free pyridine is indicated with **orange ▲**

Figure S3. ^{1}H-^{1}H NOESY 2S NMR spectrum for an irradiated solution of [(p-cymene)Ru(bpm)(py)]$^{2+}$ + 9-ethylguanine in D_2O (aromatic region: zoom). Irradiation details: white light (400–600 nm, 1 J/cm^{2}·h) at 310 K for ca. 360 min.

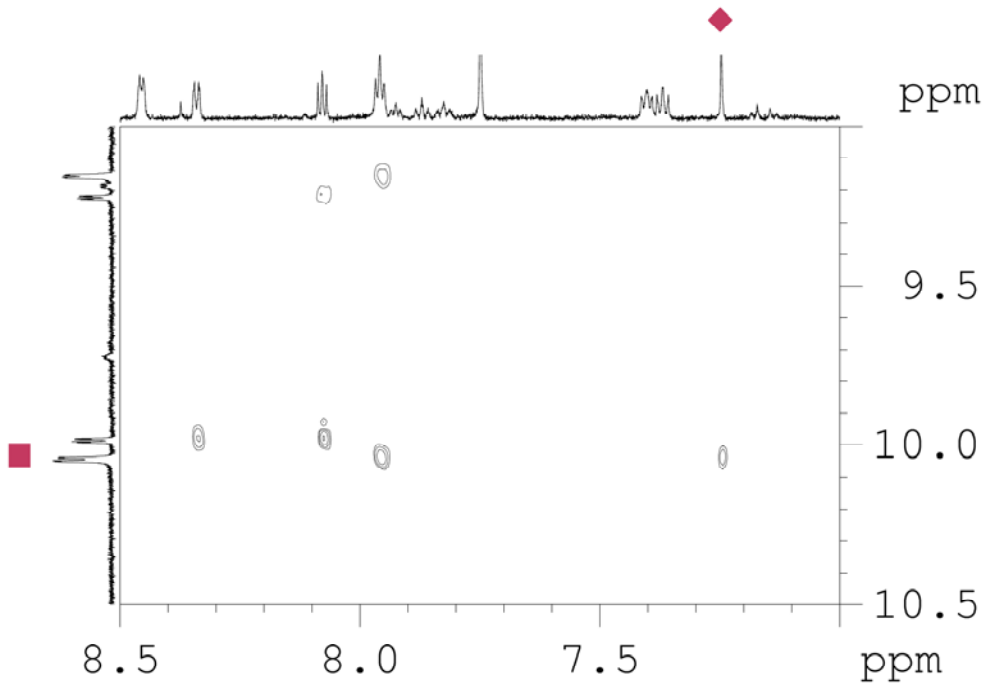

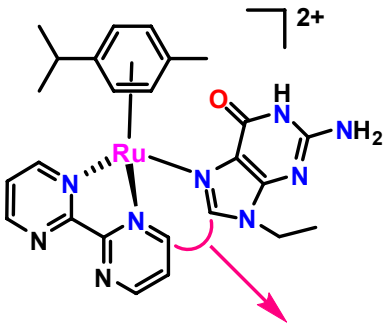

NOE cross-peak between H(8) of 9-EtG and the 2,2'-CH of bpm

Computational methods

All calculations were performed with the Gaussian 03 (G03) program[1] employing the DFT method, Becke three parameter hybrid functional and Lee-Yang-Parr's gradient corrected correlation functional[2] (B3LYP). The LanL2DZ basis set[3] and effective core potential were used for the Ru atom and the 6-31G** basis set[4] was used for all other atoms. Geometry optimizations of $[Ru(p\text{-cymene})(bpm)(py)]^{2+}$ in the ground state (S_0) and lowest-lying triplet state (T_1) were performed in the gas phase and the nature of all stationary points was confirmed by normal mode analysis. The conductor-like polarizable continuum model method (CPCM)[5] with water as solvent was used to calculate the electronic structure and the excited states of $[Ru(p\text{-cymene})(bpm)(py)]^{2+}$ in solution. Fifty singlet excited states and the corresponding oscillator strengths were determined with a Time-dependent Density Functional Theory (TDDFT)[6] calculation. The computational results are summarized in the following tables, where only selected electronic transitions. Eight triplet excited states were calculated by TDDFT starting either from the ground-state geometry or the lowest-lying triplet state geometry. The electronic distribution and the localization of the singlet and triplet excited states were visualized using the electron density difference maps (EDDMs).[7] GaussSum 1.05[8] was used for EDDMs calculations and for the electronic spectrum simulation.

1. Frisch, M. J.; et al. *Gaussian 03*, revision D 0.1; Gaussian Inc.: Wallingford CT, 2004.
2. a) Becke, A. D. *J. Chem. Phys.* **1993**, *98*, 5648-5652; b) Lee, C.; Yang, W.; Parr, R. G. *Phys. Rev. B* **1988**, *37*, 785-789.
3. Hay, P. J.; Wadt, W. R. *J. Chem. Phys.* **1985**, *82*, 270-283.
4. McLean, A. D.; Chandler, G. S. *J. Chem. Phys.* **1980**, *72*, 5639-5648.
5. Cossi, M.; Rega, N.; Scalmani, G.; Barone, V. *J. Comput. Chem.* **2003**, *24*, 669-681.
6. a) Casida, M. E.; Jamorski, C.; Casida, K. C.; Salahub, D. R. *J. Chem. Phys.* **1998**, *108*, 4439-4449; b) Stratmann, R. E.; Scuseria, G. E.; Frisch, M. J. *J. Chem. Phys.* **1998**, *109*, 8218-8224.
7. Browne, W. R.; O'Boyle, N. M.; McGarvey, J. J.; Vos, J. G. *Chem. Soc. Rev.* **2005**, *34*, 641-663.
8. O'Boyle, N. M.; Vos, J. G. *GaussSum*, Dublin City University. Available at http://gausssum.sourceforge.net., 2005.

Table S1. Selected calculated bond distances (Å) for the complex $[(p\text{-cymene})Ru(bpm)(py)]^{2+}$

	Ground-State Geometry	Lowest-Lying Triplet Geometry
Ru–N(py)	2.151	2.108
Ru–N(bpm)	2.117	2.158
Ru–N(bpm)	2.115	2.452
Ru–Arene (centroid)	1.852	2.089

Table S2. Selected TDDFT singlet transitions for the complex $[(p\text{-cymene})Ru(bpm)(py)]^{2+}$

	Energy (eV)	Wavelength (nm)	Oscillator Strength	Major contributions
1	2.8012	442.61	0.0024	HOMO→L+1 (46%) HOMO→L+3 (20%)
2	3.011	411.77	0.0059	H-2→L+3 (-15%) H-1→L+3 (34%)
3	3.0392	407.95	0.001	H-1→L+1 (21%) H-1→L+3 (13%) HOMO→L+1 (-12%) HOMO→L+2 (10%) HOMO→L+3 (14%) HOMO→L+4 (-12%)
4	3.1191	397.5	0.001	H-2→L+1 (32%) H-2→L+2 (-10%) H-2→L+4 (13%) H-1→L+1 (14%)
5	3.1993	387.54	0.0027	HOMO→LUMO (75%)
6	3.3581	369.21	0.0365	H-1→LUMO (79%)
8	3.6553	339.19	0.0148	H-2→LUMO (41%) H-2→L+3 (16%)
9	3.7767	328.28	0.0108	H-2→LUMO (48%) H-2→L+3 (-25%)
13	4.1763	296.88	0.0804	H-1→L+2 (13%) HOMO→L+4 (54%)
14	4.2527	291.54	0.0081	H-3→LUMO (16%) H-1→L+4 (59%)
16	4.4026	281.62	0.0051	H-7→LUMO (29%) H-6→LUMO (61%)
17	4.5092	274.96	0.0076	H-2→L+2 (19%) HOMO→L+5 (68%)
18	4.5221	274.18	0.0085	H-2→L+1 (10%) H-2→L+2 (43%) H-2→L+3 (-10%) HOMO→L+5 (-23%)
21	4.6758	265.16	0.0494	H-1→L+5 (83%)
22	4.7048	263.53	0.0652	H-5→LUMO (19%) H-4→L+2 (-17%) HOMO→L+7 (-14%)
23	4.7188	262.74	0.0369	H-1→L+6 (-18%) HOMO→L+7 (31%)
24	4.782	259.27	0.0807	H-5→LUMO (-12%) H-3→L+1 (13%) H-1→L+6 (-12%) H-1→L+7 (18%)
25	4.79	258.84	0.0006	H-3→L+1 (58%)

				H-3→L+3 (18%) H-1→L+6 (10%)
26	4.8081	257.86	0.1692	H-5→LUMO (18%) H-1→L+6 (-11%) H-1→L+7 (18%)
27	4.8323	256.57	0.0219	H-6→L+2 (-12%) H-4→L+4 (24%)
28	4.9095	252.54	0.0166	H-7→LUMO (61%) H-6→LUMO (-29%)
31	5.0629	244.89	0.0323	H-4→L+1 (24%) H-1→L+7 (-10%)
32	5.1086	242.7	0.0425	H-2→L+5 (60%)
33	5.1112	242.57	0.0231	H-5→L+1 (-18%) H-2→L+5 (21%) H-2→L+6 (-17%)
38	5.2545	235.96	0.0378	H-8→LUMO (33%) H-5→L+2 (-13%) H-4→L+2 (13%)
43	5.3589	231.36	0.0463	H-7→L+3 (-11%) H-6→L+2 (14%)

Table S3. Selected Electron Difference Density Maps (EDDMS) of singlet excited state transitions of $[(p\text{-cymene})Ru(bpm)(py)]^{2+}$ in H_2O (light violet indicates a decrease in electron density, while purple indicates an increase)

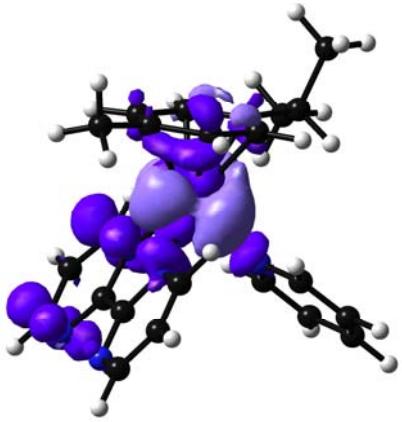 **S1**	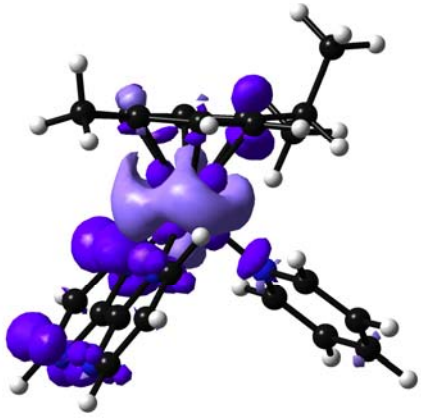 **S2**	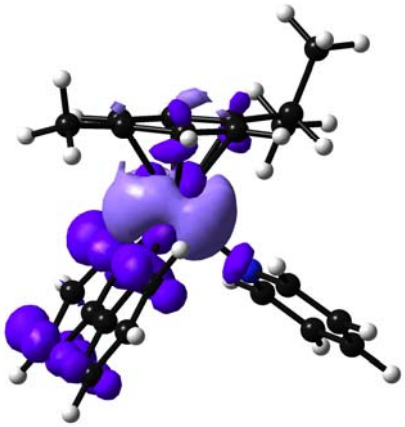 **S3**
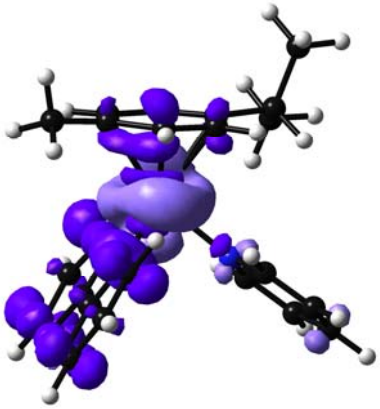 **S4**	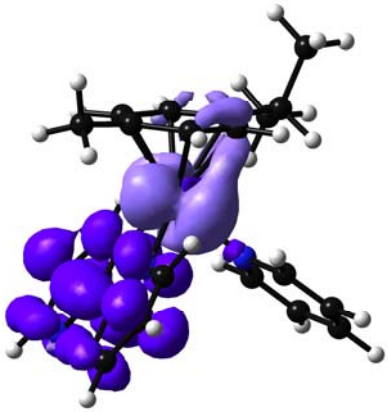 **S5**	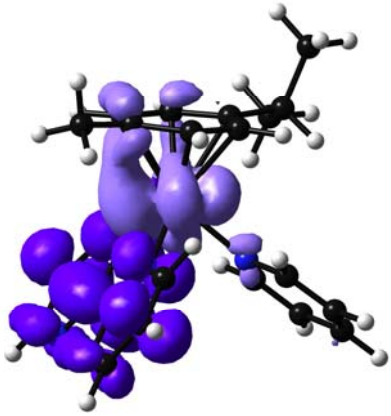 **S6**

Table S4. Selected TDDFT triplet transitions for the complex [(p-cymene)Ru(bpm)(py)]$^{2+}$ in the ground-state optimized geometry

	Energy (eV)	Wavelength (nm)	Oscillator Strength	Major contributions
1	2.252	550.56	0.0	HOMO->L+1 (74%) HOMO->L+3 (21%)
2	2.4005	516.5	0.0	HOMO->L+2 (17%) HOMO->L+3 (45%) HOMO->L+4 (-23%)
3	2.4861	498.71	0.0	H-1->L+1 (69%) H-1->L+3 (19%)
4	2.5342	489.24	0.0	H-2->L+1 (-13%) H-1->L+2 (12%) H-1->L+3 (48%) H-1->L+4 (-16%)
5	2.7133	456.94	0.0	H-2->L+1 (58%) H-2->L+2 (-10%) H-2->L+4 (14%)
6	2.8504	434.97	0.0	H-2->L+3 (69%)
7	2.9257	423.78	0.0	H-5->LUMO (-18%) HOMO->LUMO (71%)
8	3.1334	395.68	0.0	H-1->LUMO (86%)

Table S5. Selected Electron Difference Density Maps (EDDMS) of triplet excited state transitions of [(p-cymene)Ru(bpm)(py)]$^{2+}$ in H_2O (pink indicates a decrease in electron density, while red indicates an increase). Calculations were performed using the ground-state optimized geometry

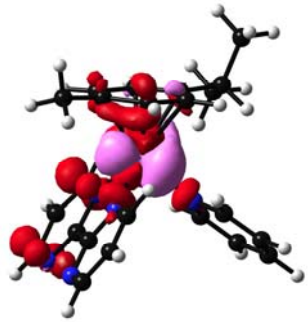 **T1**	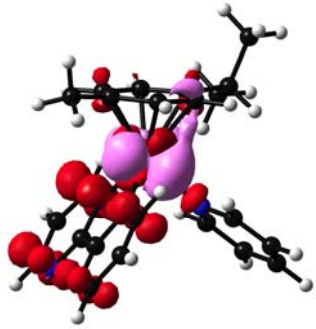 **T2**	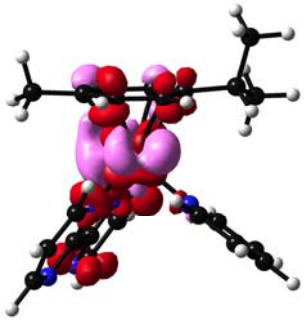 **T3**
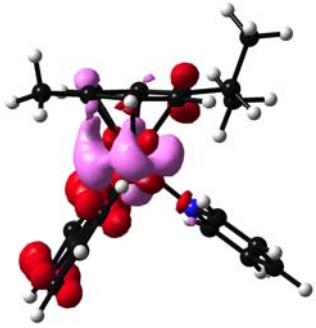 **T4**	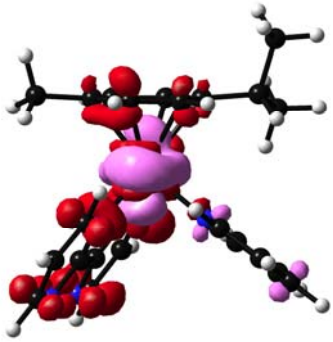 **T5**	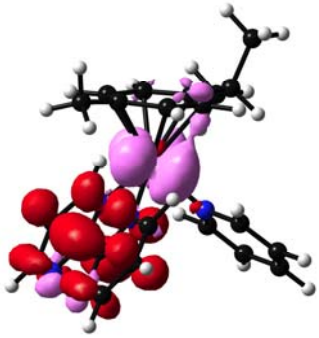 **T6**
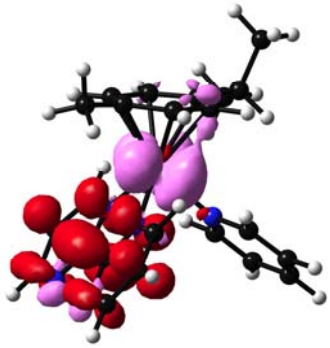 **T7**	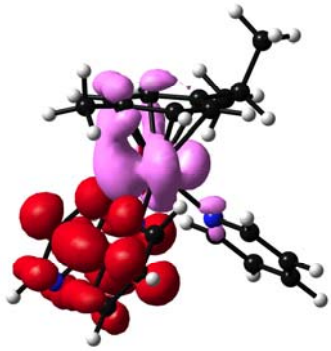 **T8**	

Table S6. Selected TDDFT triplet transitions for the complex [(p-cymene)Ru(bpm)(py)]$^{2+}$ in the lowest-lying triplet-state optimized geometry

	Energy (eV)	Wavelength (nm)	Oscillator Strength	Major contributions
1	0.6484	1912.14	0.0	H-1->LUMO (125%) HOMO->LUMO (59%)
2	0.8057	1538.84	0.0	H-1->LUMO (-53%) HOMO->LUMO (98%)
3	1.0691	1159.74	0.0	H-2->LUMO (134%)
4	1.8923	655.21	0.0	HOMO->L+2 (101%)
5	2.1397	579.46	0.0	H-1->L+2 (99%)
6	2.4765	500.64	0.0	H-2->L+2 (96%)
7	2.9304	423.09	0.0	H-5->L+1 (16%) HOMO->L+1 (83%)
8	3.2859	377.32	0.0	H-1->L+1 (86%)

The energy values of the triplet transitions in the Table are calculated relatively to the energy of the lowest-lying geometry computed with multiplicity equal to 1 (singlet). To calculate the relative energy of these triplet states with respect to the ground state, 0.97 eV must be added.

Table S7. Selected Electron Difference Density Maps (EDDMS) of triplet excited state transitions of [(p-cymene)Ru(bpm)(py)]$^{2+}$ in H_2O (pink indicates a decrease in electron density, while red indicates an increase). Calculations were performed using the lowest-lying triplet-state optimized geometry.

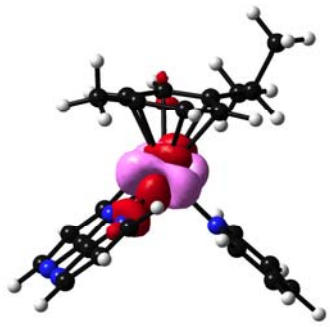 **T1**	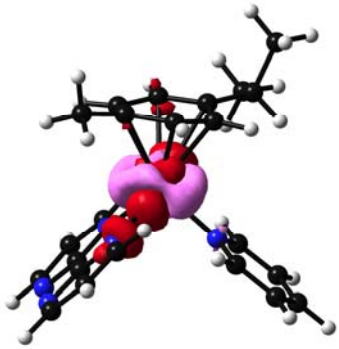 **T2**	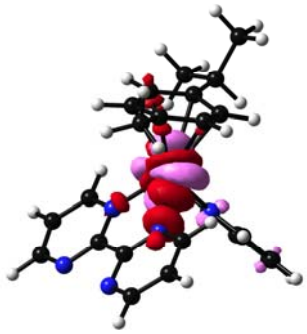 **T3**
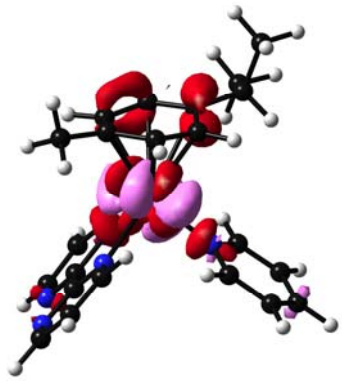 **T4**	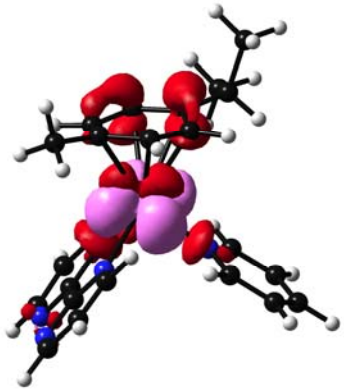 **T5**	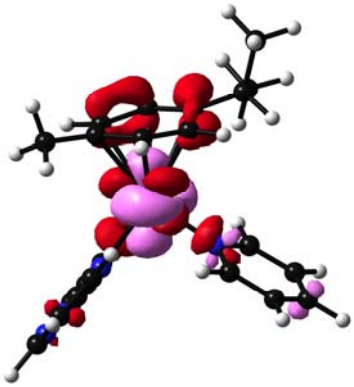 **T6**
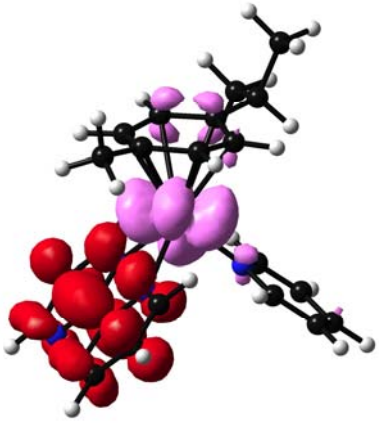 **T7**	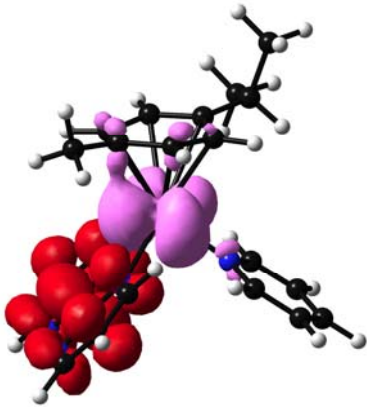 **T8**	

Figure S4. Excited-state energy diagram for $[(p\text{-cymene})Ru(bpm)(py)]^{2+}$

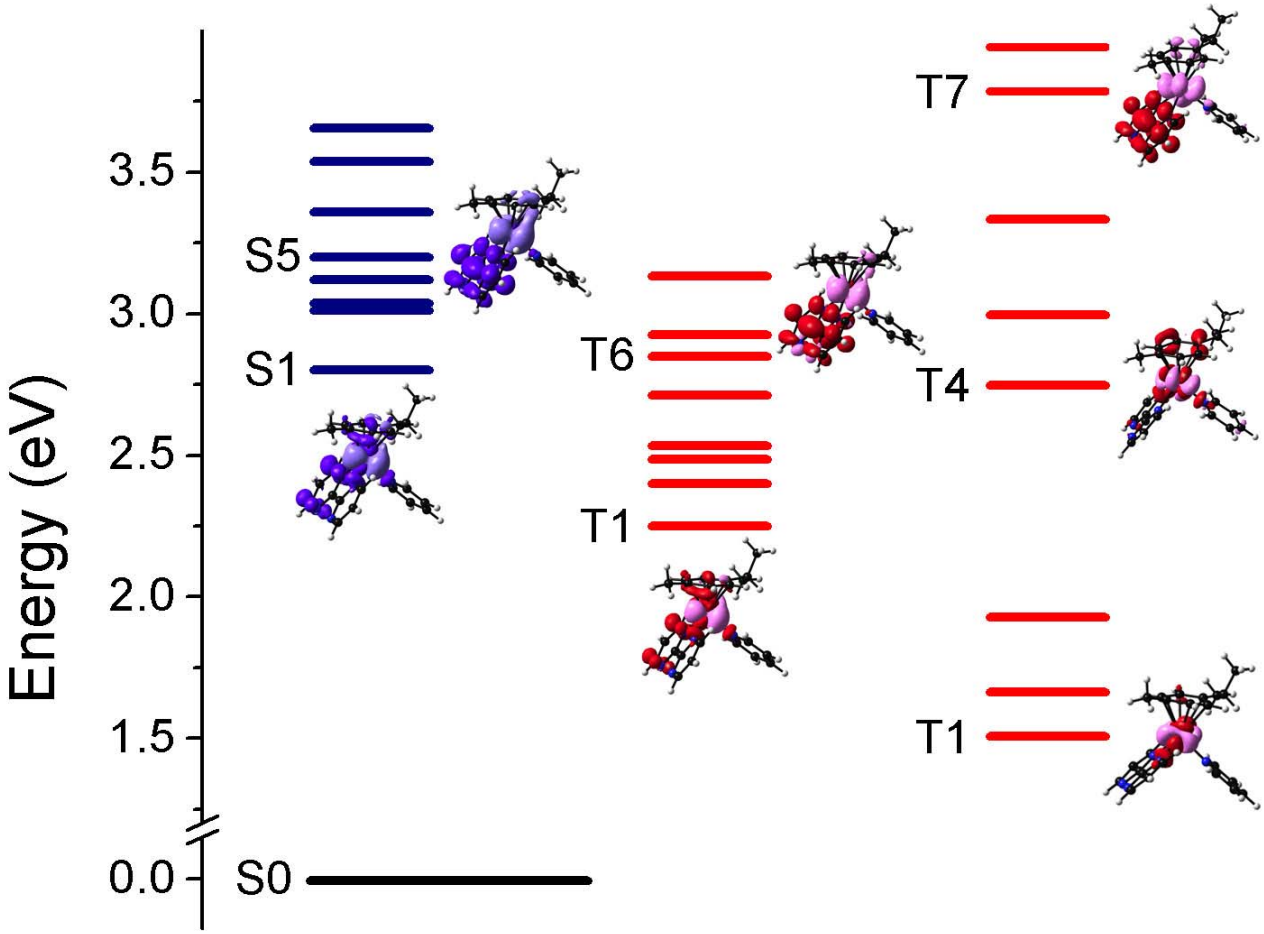

Figure S5. Selected orbitals (isovalue 0.02) for $[(p\text{-cymene})Ru(bpm)(py)]^{2+}$ for the ground-state optimized geometry

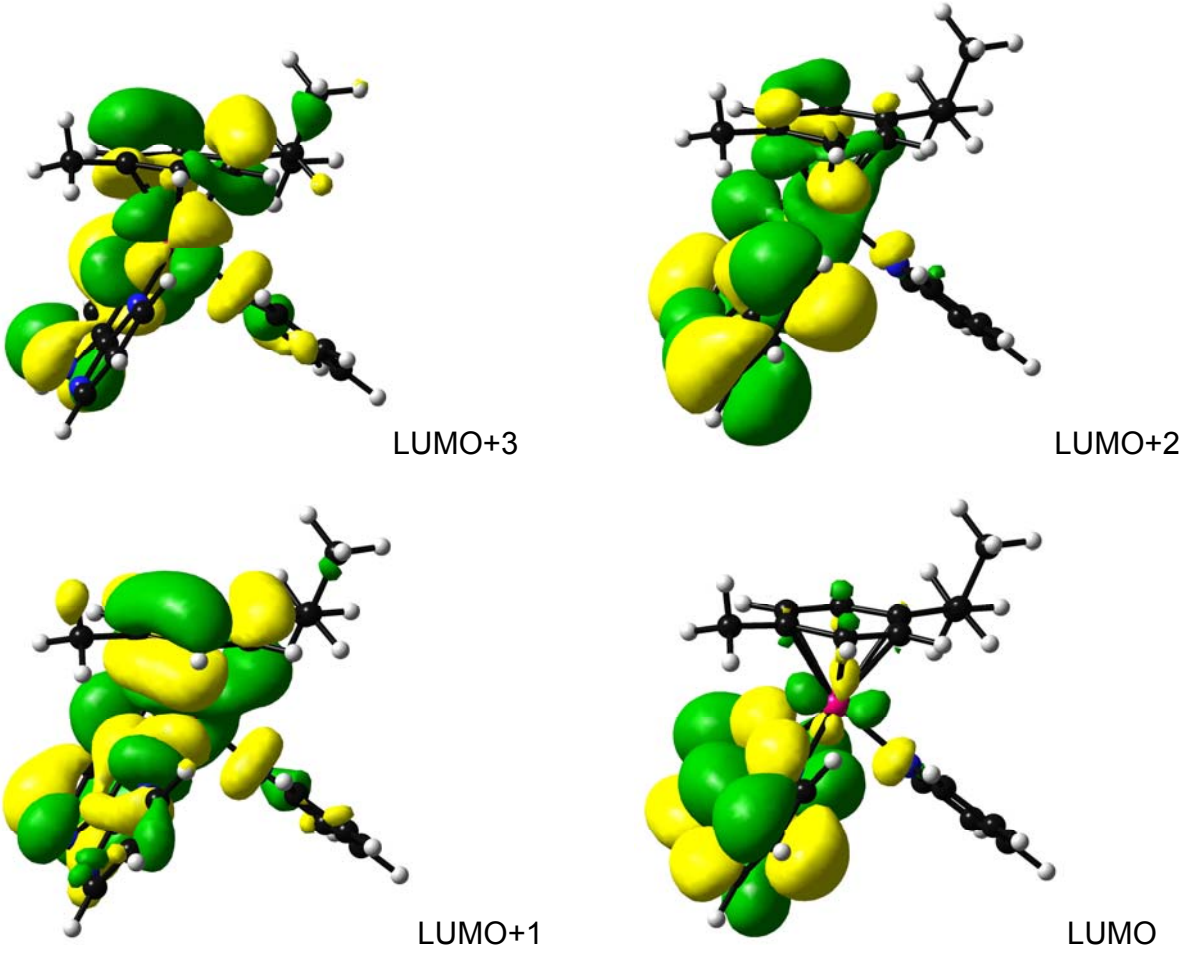

Figure S6. Selected orbitals (isovalue 0.02) for $[(p\text{-cymene})Ru(bpm)(py)]^{2+}$ for the lowest-lying triplet optimized geometry

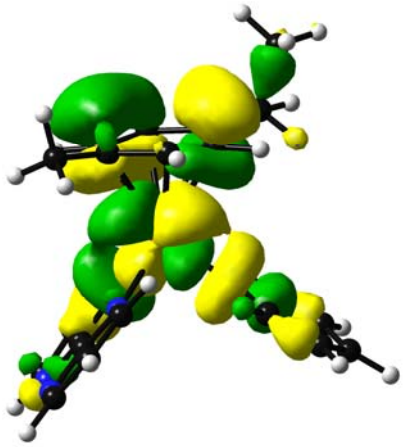

LUMO α

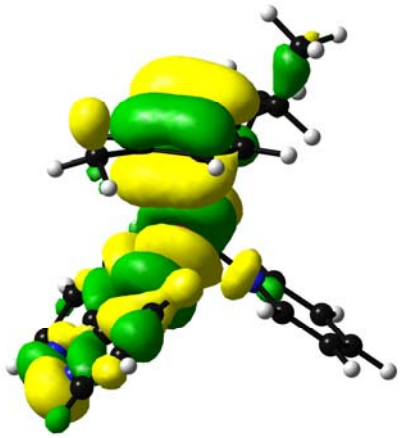

h-SOMO

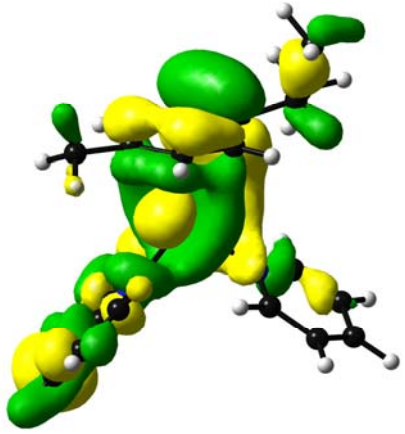

l-SOMO

Figure S7. Speciation graph of the photoconversion of **1a** into **1b**. Irradiation details: white light (400–600 nm, 1 J/cm^2·h) at 310 K for 425 min.